



ÄSPÖLABORATORIET

**INTERNATIONAL
COOPERATION
REPORT**

94-07

**Analyses of LPT2 in the Äspö HRL
with continuous anisotropic
heterogeneous model**

Akira Kobayashi¹, Ryo Yamashita², Masakazu
Chijimatsu², Hiroyuki Nishiyama³, Yuzo Ohnishi³

- 1 Iwate University, Iwate, Japan
- 2 Hazama Corporation, Ibaraki, Japan
- 3 Kyoto University, Kyoto, Japan

September 1994

Supported by PNC, Japan

SVENSK KÄRNBRÄNSLEHANTERING AB
SWEDISH NUCLEAR FUEL AND WASTE MANAGEMENT CO

BOX 5864 S-102 40 STOCKHOLM

TEL. +46-8-665 28 00 TELEX 13108 SKB TELEFAX +46-8-661 57 19

9505310292 950424
PDR WASTE
WM-11 PDR

ANALYSES OF LPT2 IN THE ÄSPÖ HRL WITH CONTINUOUS ANISOTROPIC HETEROGENEOUS MODEL

*Akira Kobayashi¹, Ryo Yamashita², Masakazu Chijimatsu²,
Hiroyuki Nishiyama³, Yuzo Ohnishi³*

- 1 Iwate University, Iwate, Japan**
- 2 Hazama Corporation, Ibaraki, Japan**
- 3 Kyoto University, Kyoto, Japan**

September 1994

Supported by PNC, Japan

This document concerns a study which was conducted within an Äspö HRL joint project. The conclusions and viewpoints expressed are those of the author(s) and do not necessarily coincide with those of the client(s). The supporting organization has reviewed the document according to their documentation procedure.

102.8

**Analyses of LPT2 in the Äspö HRL with
Continuous Anisotropic Heterogeneous Model**

September, 1994

Akira Kobayashi

Iwate University, Iwate, Japan

Ryo Yamashita and Masakazu Chijimatsu

Hazama Corporation, Ibaraki, Japan

Hiroyuki Nishiyama and Yuzo Ohnishi

Kyoto University, Kyoto, Japan

Contents

EXECUTIVE SUMMARY	II
INTRODUCTION	1
INFERENCE FRACTURE GEOMETRY	2
Theory	2
Application to HRL Test Site	5
ESTIMATION OF REPRESENTATIVE ELEMENTARY VOLUME	10
Crack tensor theory by Oda(1986)	10
Application to HRL Test Site	12
Estimation of α_{ij}	13
SEEPAGE AND TRANSPORT ANALYSES	17
Model Description	17
Results of Flow Analyses	20
Results of Transport Analyses	23
CONCLUSIONS	31
REFERENCES	34
APPENDIX	
A: Model and Code Specification	35
B: Main data used in the model	38

EXECUTIVE SUMMARY

The methods to model flow in a fractured rock mass can be roughly divided into a discontinuous approach and an equivalent continuous one. In this report, an equivalent continuous approach is tested. Among many equivalent approaches, the Crack tensor theory, which has been proposed by Oda (1986), is used to treat a number of fractures and to examine the dependency of the parameters on volume. Moreover, the equivalent continuous medium is modeled by a stochastic method to present the heterogeneity of the medium. For modeling of Äspö test site, the large certain fracture zones, i.e., EW3, NE2 and EW1, are presented by two dimensional plane elements of which location is decided according to the geological conceptual model. On the other hand, a series of NNW fracture zones and EW5, the probably confirmed fracture zones, are modeled by the equivalent continuous approach.

The following steps are carried out to make a continuous heterogeneous model for the probably confirmed fracture zones. Figure 1 shows the flow-chart of the analysis. Firstly, the probability model of fracture length and fracture density, which are difficult to measure in the field, are inferred from the observed data. The newly developed method is introduced. Secondly the representative elementary volume (REV) is examined by using the theory by Oda, called the Crack tensor theory in this report, with the information of fracture geometry. This is because the dependency of the results on the mesh size is avoided. The permeability has to be fundamentally defined from the solution of the boundary value problem and has to be considered as the value at a point to apply the geostatistics method.

Thirdly, the permeability corresponding to the REV is derived from the field test data by using the arithmetic and geometric averaging methods. Fourthly, the heterogeneity of the medium is represented by the conditional simulation of the geostatistical approach. In this approach, the mechanical dispersion phenomena are understood to be caused from the heterogeneous velocity vector distribution due to the heterogeneous permeability field. So a macro-dispersion phenomenon is expressed by the random process in the model. Lastly, the flow and transport analyses are carried out for each realized medium and the comparison with measured data are performed. The breakthrough curve is calculated by the ensemble of the arrival time of the particles of each realized model.

As the results, it is found that the probability density function of the fracture length can be estimated to be a log normal distribution and the representative elementary volume of the Äspö area is estimated to be about 30m cube. Moreover, it is also found better that the permeability measured at a single borehole test is averaged using an arithmetic mean rather than the geometric mean. Since the arithmetic mean can reflect an odd value, it is inferred that the measured high permeability has much effect on the permeability of the volume of REV. This may mean good connectivity of the high permeability parts. For

flow analyses, the drawdown of the head measured at observation holes are well simulated by the calculation using the permeability averaged with an arithmetic mean as shown in Figure 2. The flow rate through a hole is underestimated by the calculation. The calculated maximum flow rate has a better agreement with the measured results. For transport analyses, the calculated breakthrough curve has a relatively good agreement with the measured ones as shown in Figure 3. However, the breakthrough curve can be calculated for the tracer which was not measured in the field because the tracer is moving into the pumping-up hole in the simulation.

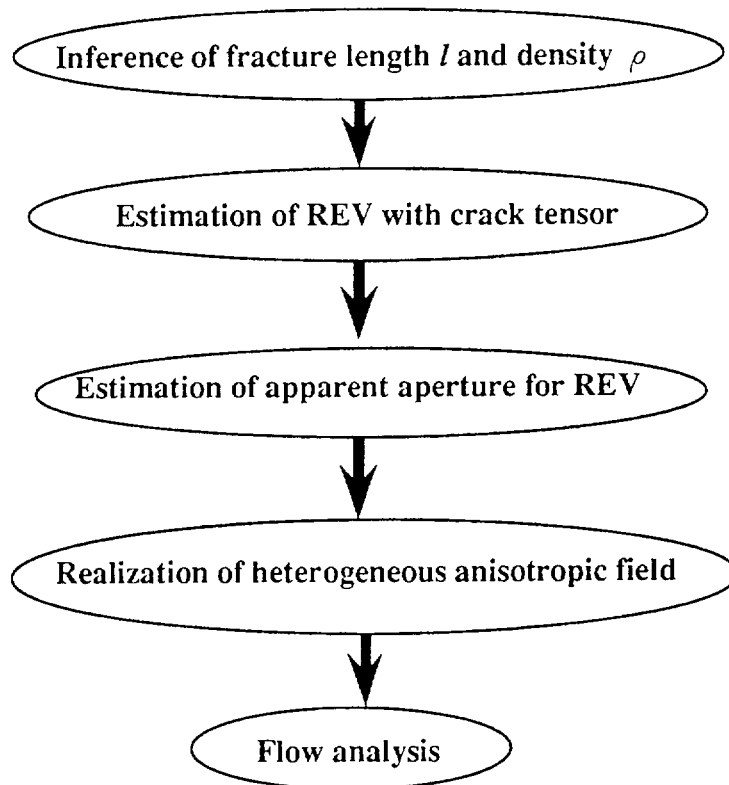


Figure 1 Analysis flow-chart

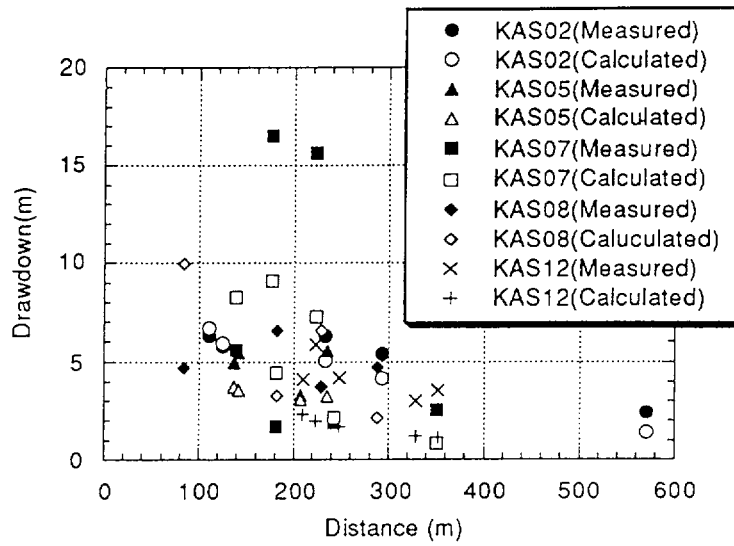
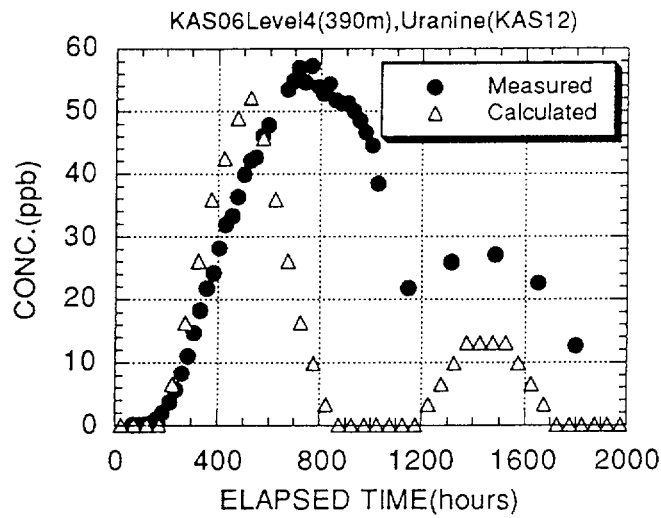


Figure 2 Comparison between calculated and measured drawdown



(b) Comparison of the level 14 (390m)

Figure 3 Calculated and measured breakthrough curve for the test from KAS12

INTRODUCTION

The methods to model flow in a fractured rock mass can be roughly divided into a discontinuous approach and an equivalent continuous one. The representatives of discontinuous approaches are the ones by Dershowitz et al (1991). and Herbert et al. (1990), which have been tested in the STRIPA project. These methods are proved to be very effective for relatively small region, e.g., a few hundreds meters cubic. However, it would be difficult for these methods to model a relatively large region, e.g., a few kilo meters cubic because of the limitation of the computer capacity. For such a case, the modeled fractures have to be selected by some criteria in order to reduce the number of those. This selection process may be a little ambiguous. A subjective judgement may be necessary for the selection to validate the model applicability. Applicability of the discontinuous approach for a large region will be tested by the other group of Power Reactor and Nuclear Fuel Development Corporation (PNC) with a corporation of Golder Associates. This is very important issue for a performance assessment of radioactive waste disposal project. In this report, an equivalent continuous approach is tested. Among many equivalent approaches, the Crack tensor theory, which has been proposed by Oda (1986), is used because this is very convenient to treat a number of fractures and to examine the dependency of the parameters on volume. This method can consider the information of fracture geometry similarly to the discontinuous approach. For modeling of Äspö test site, the large certain fracture zones, i.e., EW3, NE2 and EW1, are presented by two dimensional plane elements of which location is decided according to the conceptual model. On the other hand, a series of NNW fracture zones and EW5 are probably confirmed, while the location of those fractures is represented decisively in the conceptual model made by SKB. As a matter of fact, many fractures regarded as these probably confirmed ones can be observed on the outcrops, and it is difficult to identify the locations of each fractures as a concentrated fractured zone. Thus, these probably confirmed fractures are modeled by the equivalent continuous approach. Moreover, the equivalent continuous medium is modeled by a stochastic method to represent the heterogeneity of the medium. A few steps are necessary to make a continuous heterogeneous model.

Firstly, the probability model of fracture length and fracture density, which are difficult to measure in the field, are inferred from the observed data. The newly developed method is introduced. Secondly the representative elementary volume (REV) is examined by using the theory by Oda, called the Crack tensor theory in this report, with the information of fracture geometry. Thirdly, the permeability corresponding to the REV is derived from the field test data. Fourthly, the heterogeneity of the medium is represented by the conditional simulation of the geostatistical approach. Lastly, the flow and transport analyses are carried out for each realized medium and the comparison with measured data are performed. The process of the analyses are briefly shown in Figure 1.

It is noted that the heterogeneity of the medium is modeled as a random process in this approach.

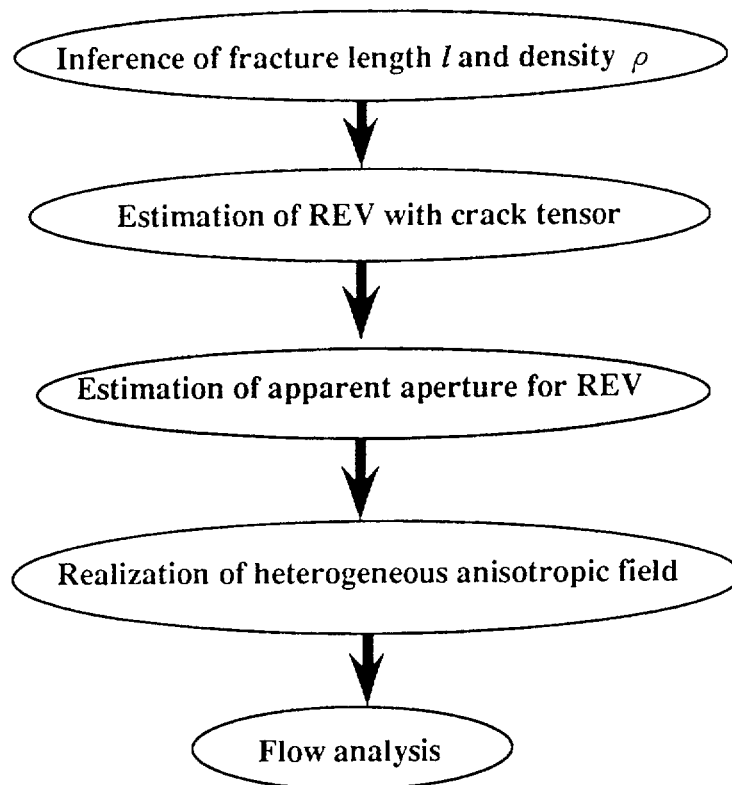


Figure 1 Analysis flow-chart

INFERENCE OF FRACTURE GEOMETRY

Theory

Before realizing the fracture structure, it is necessary to derive the statistical information of fracture geometry from the measured data. Among fracture geometry, fracture length is difficult to measure at the field surveys. It is usual to infer the fracture length by assuming the shape of fractures and the pdf of the fracture length, and by comparing estimated trace length information with measured one (Dershowitz, et al. (1991)). Although the presented approach is based on the similar concept, more systematic way is introduced.

Consider an entire region defined by the borehole length, L , and the area, A , normal to the borehole direction as shown in Figure 2. The volume of the entire region is given by $V = AxL$. Now, assume that M fractures exist in the volume of V and N fractures among them are penetrated by a given borehole. The projected area of a fracture having the area of a on the plane A is presented by a_f . The probability that a fracture is penetrated by the borehole is given by a_f/A . Thus, multiplying the total number of the fractures by this probability, the number of the fractures penetrated by the borehole is obtained by

$$N = \frac{a_f}{A} M = \frac{a_f}{A} L A \rho = a_f L \rho \quad (1)$$

where ρ is the fracture density defined by $\rho = M/V$. Thus, the fracture density is given as

$$\rho = \frac{N}{La_f} \quad (2)$$

in which N/L is the fracture frequency observed at a borehole.

Giving the angle, θ , between fracture plane and plane A , a_f can be written as

$$a_f = a \cos \theta. \quad (3)$$

Assuming that the shape of a fracture is a circle of which diameter is r , the equation (3) can be rewritten as

$$a_f = a \cos \theta = \frac{\pi r^2}{4} \cos \theta \quad (4)$$

where $\cos \theta$ is given as the internal product of the unit vector of borehole direction, \mathbf{b} , and the unit normal vector of a fracture, \mathbf{n} , i.e., $\cos \theta = \mathbf{n} \cdot \mathbf{b}$.

The square of the fracture diameter, i.e., fracture length, in the equation (4) is given by the expectation of the fracture length, which is dependent on the probability density function (pdf), f , of the fracture length.

$$\langle (r^k)^2 \rangle = \int_0^{\infty} r^2 f(r^k) dl \quad (5)$$

Thus, the a_f matrix is given as

$$[a_f]^{km} = \frac{\pi}{4} E \langle (r^k)^2 \rangle [\cos \theta]^{km}. \quad (6)$$

Using the assumed probability parameters, $E((r^k)^2)$ is calculated.

However, it is difficult to measure the pdf of the fracture length as a matter of fact. The calculation of the equation (6) has to be carried out with the assumed pdf of the fracture length and its parameters. From the above process, the fracture density can be inferred from the fracture frequency observed at a borehole, the borehole direction and the fracture direction with an assumed probability model of the fracture length.

Then, the fracture geometry is reproduced by using the above fracture information. The mean trace length and the variance corresponding to the outcrops are calculated and compared with the observed ones. By calibrating the probability model of the fracture length, the best pdf of the fracture length and its parameters are finally decided. It is possible through the above process to get the fracture density, the pdf of the fracture length and its parameters consisting to the observed results at both boreholes and outcrops. Figure 3 shows the above process schematically.

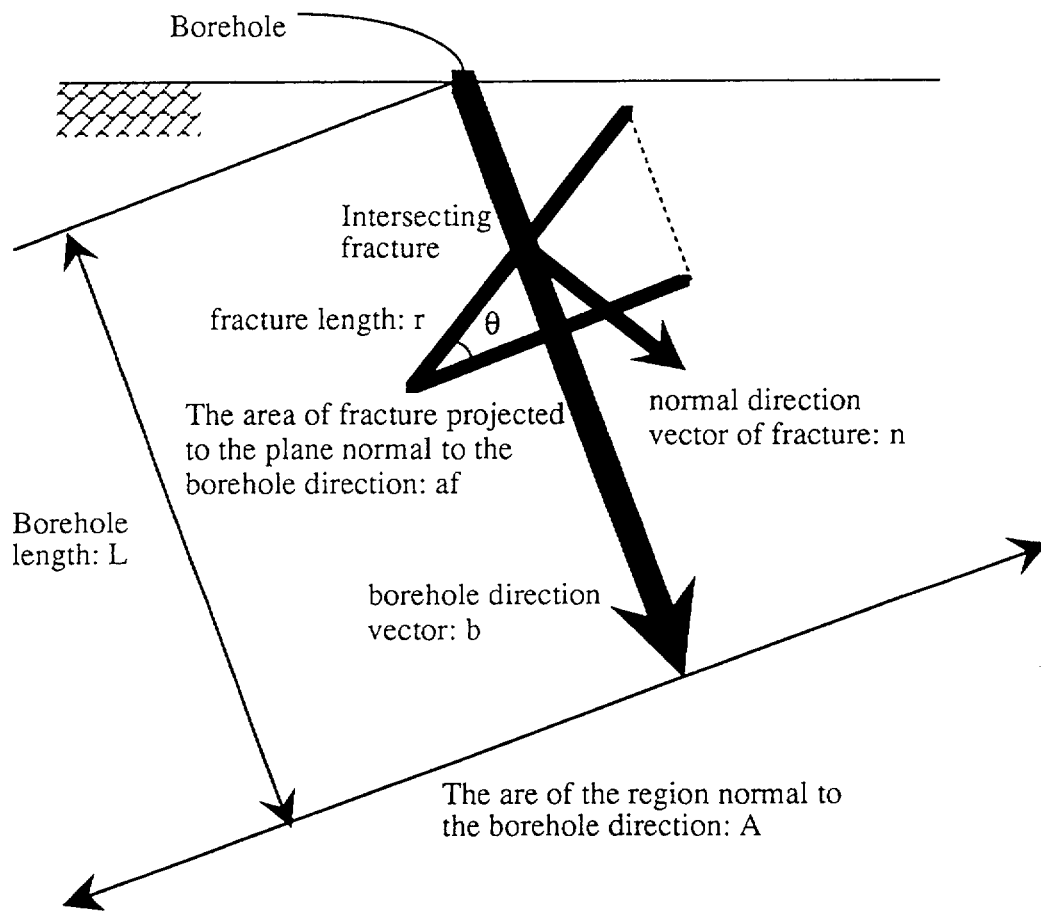


Figure 2 Schematic view of the relation between a boreholes and the intersecting fracture

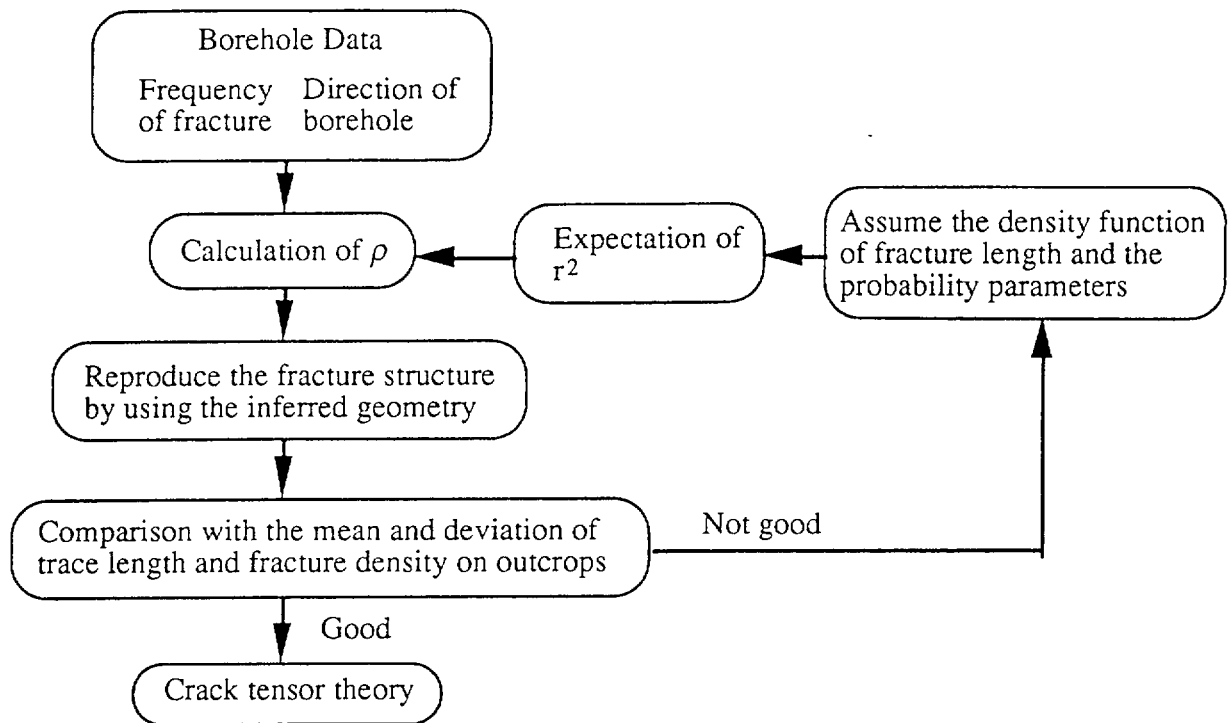


Figure 3 Flow of decision of pdf of fracture length and density

Application to HRL Test Site

The fracture frequency at the boreholes is observed at HRL test site while the direction information of each fracture in a borehole is not measured. Thus, the above theory is applied by assuming that the fracture density is homogeneous in a space and is different between fracture sets. In this case, the equation can be written in a matrix form as

$$\left[\frac{N}{L}\right]^m = [a_j]^{km} [\rho]^k \quad (7)$$

where the superscript, m , indicates the number of boreholes and k is the number of fracture sets. $[N/L]^m$ is the vector of the fracture frequency observed at the boreholes, $[a_j]^{km}$ is the matrix obtained from the equation (6). By solving this matrix equation, the fracture density is obtained for each fracture set. In the case where the number of the boreholes is less than that of the fracture sets, this approach is difficult to apply. On the other hand, when the number of the boreholes is larger than that of the fracture sets, the equation can be solved by using the least square method.

The fracture frequency is observed at 11 boreholes, i.e., KAS03-09, KAS11-14. Table 1 shows the fracture frequency and the borehole direction of each borehole. The borehole direction is calculated by using the reference axis, i.e., x-axis is corresponding to the north direction, y-axis is the west direction and z-axis is upward direction.

The fractures are observed on the outcrops. It can be seen from the observed fracture geometry on the outcrops that the dominant strike of the fractures is N30°E, N30°W, N80°E and N80°W and the dominant dip is 80°E, 80°W, 20°E and 20°W. These fracture sets may be corresponding to a series of NNW and EW-5. Thus, the fracture sets used in the analyses are assumed to be classified into 8 sets as shown in Table 2. By using the both fracture directions in Table 1 and fracture sets in Table 2, $\cos\theta$ in the equation (6) is calculated.

Then, the probability property of the fracture length is assumed for each fracture set. In this report, the log normal, exponential and Gamma distribution are examined as a pdf of fracture length. The expectation of r^2 in the equation (5) is analytically calculated for the exponential and Gamma function as follows;

Exponential distribution:

$$\text{pdf: } P(r) = \frac{1}{r_0} e^{-\frac{r}{r_0}}$$

$$E(r^2) = \int_0^{\infty} r^2 P(r) dr = 2r_0^2 \quad (8)$$

Gamma distribution:

$$\text{pdf: } P(r) = \frac{r}{r_0} e^{-\frac{r}{r_0}}$$

$$E(r^2) = \int_0^{\infty} r^2 P(r) dr = 6r_0^2 \quad (9)$$

On the other hand, $E(r^2)$ for the log normal distribution is numerically calculated in a computer code because it is difficult to derive analytically the expectation of r^2 . By using $E(r^2)$ and $\cos\theta$, the matrix $[a_{ij}]^{km}$ is calculated as shown in the equation (6). Then, the fracture density for each fracture set is calculated by solving the equation (7).

Next, the fracture geometry is reproduced in the region of 10m cube with the fracture information obtained by the above process, and the volume is intersected at the center level by the horizontal plane pretending the outcrops. The area of the plane is similar to that of the outcrops and the most outcrops are horizontal. The fractures on the plane, having the trace length over 50 cm, are picked up and the mean trace length, the variation and the trace fracture density (the number of traced fractures per unit area) are calculated and compared with the observed ones on the outcrops. The probability

parameters are calibrated for each pdf to get a good agreement with observed ones. Figure 4 shows the above process to examine the pdf of the fracture length. Table 3 shows the parameter values of each fracture set to give the best agreement with the measured ones and Table 4 indicates the comparison with the measured results. It can be seen from Table 4 that the log normal distribution gives the best agreement with the measured results. Thus, the log normal distribution is assumed to be the pdf of the fracture length and the mean length and the standard deviation are set at the values shown in Table 3 to examine with the Crack tensor theory.

Table 1 Borehole direction and fracture frequency

Borehole No.	Coordinate of the borehole			length (m)	Dip	Strike	Borehole direction			fracture N/L
	X	Y	Z				bx	by	bz	
KAS02	7250.11	2125.22	7.68	924	85	330	0.0755	0.0436	-0.996	no data
KAS03	7758.22	1805.20	8.79	1002	85	330	0.0755	0.0436	-0.996	3.71
KAS04	7636.82	1955.06	11.66	481	60	135	-0.354	-0.354	-0.866	6.02
KAS05	7247.97	2059.61	8.68	550	85	150	-0.075	-0.0436	-0.996	2.54
KAS06	7067.74	2175.08	5.16	602	60	335	0.498	0.0436	-0.866	3.61
KAS07	7229.66	2215.40	4.58	604	59	205	-0.467	0.218	-0.857	3.65
KAS08	7451.05	2150.44	7.66	601	60	135	-0.354	-0.354	-0.866	2.91
KAS09	6925.19	2091.11	4.08	450	60	169	-0.491	-0.0954	-0.866	4.07
KAS11	6937.02	2090.71	4.26	249	89	22	0.0102	-0.0065	-1.000	4.00
KAS12	7568.80	2156.60	4.83	380	69	150	-0.310	-0.179	-0.934	3.97
KAS13	7264.40	2169.00	3.89	406	62	267	-0.0246	0.469	-0.883	2.91
KAS14	6948.54	2138.80	3.70	212	60	137	-0.366	-0.341	-0.866	5.43

Table 2 Unit normal vector of fracture set

Fracture sets	Dip	Strike	X(N)	Y(W)	Z(up)
N30W80W	10	60	0.492	-0.853	-0.174
N30W80E	10	240	-0.492	0.853	-0.174
N30E80W	10	120	-0.492	-0.853	-0.174
N30E80E	10	300	0.492	0.853	-0.174
N80W20W	70	10	0.337	-0.0594	-0.940
N80W20E	70	190	-0.337	0.0594	-0.940
N80E20W	70	170	-0.337	-0.0594	-0.940
N80E20E	70	350	0.337	0.0594	-0.940

Table 3 Calculated mean fracture length and fracture density

Fracture sets	Log normal		Density (N/m ²)	Exponential		Gamma	
	Length Mean	St. dev.		Mean length	Density (N/m ²)	Mean length	Density (N/m ²)
N30W80W	1.0	0.8	17.8	0.3	289	0.5	4.88
N30W80E	1.0	0.8	14.4	1.2	12.2	1.2	18.9
N30E80W	1.0	0.8	22.6	0.3	325.7	0.5	5.50
N30E80E	1.0	0.8	29.1	1.2	2.45	1.2	38.2
N80W20W	0.5	0.55	16.7	0.5	190.6	1.0	35.7
N80W20E	0.5	0.55	14.5	0.5	216.5	1.0	40.6
N80E20W	0.5	0.55	11.9	0.5	218.1	1.0	40.9
N80E20E	0.5	0.55	10.8	0.5	189	1.0	35.4

Table 4 Comparison between calculated and measured trace length on the outcrops

	Mean Trace Length (m)	St. dev. of trace length (m)	Density of traced fractures (N/m ³)
Log normal	1.83	1.92	2.33
Exponential	1.51	1.42	4.65
Gamma	3.41	3.05	9.11
Mean observation	1.41	3.77	2.64

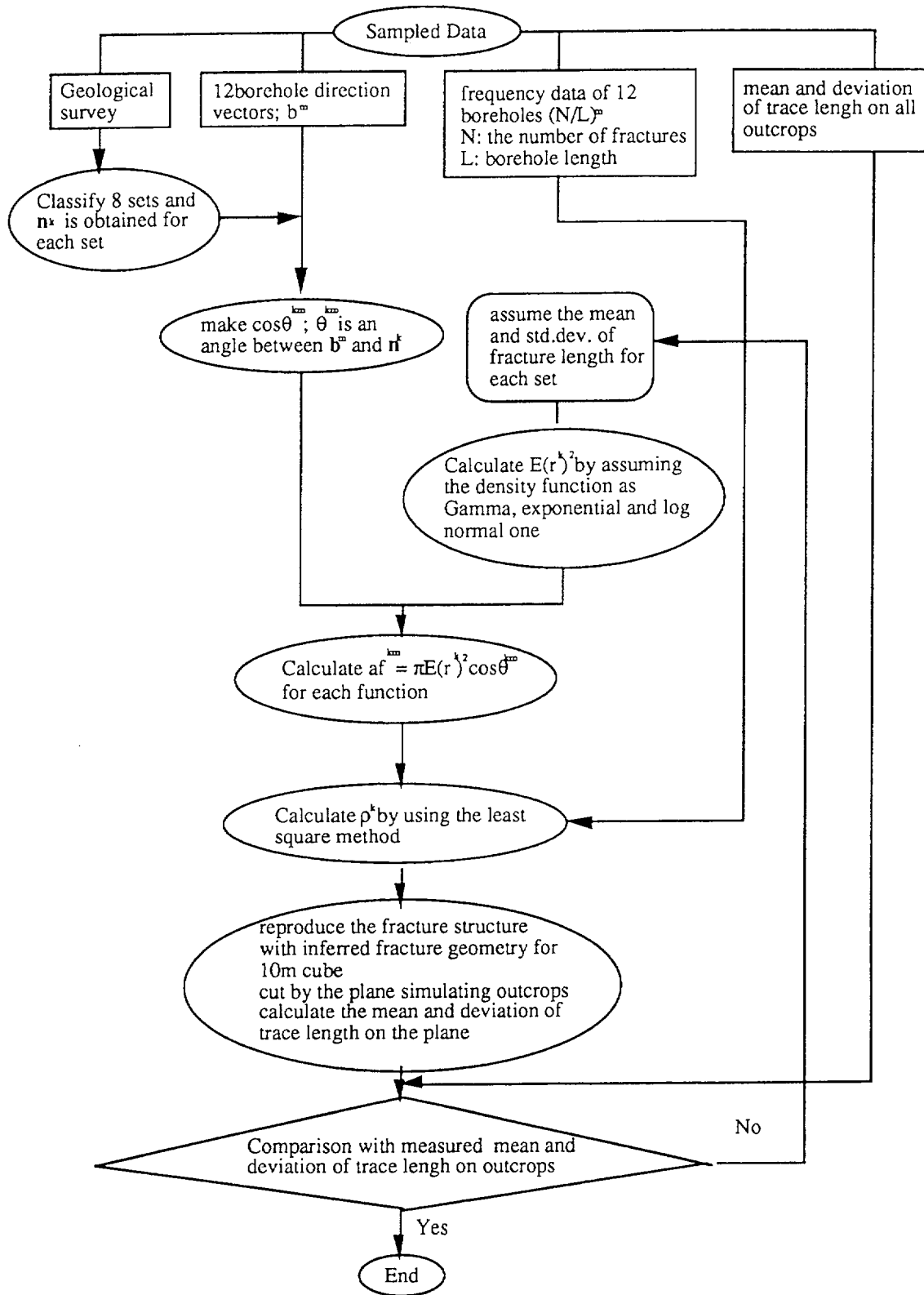


Figure 4 Process to decide fracture density and pdf of fracture length

ESTIMATION OF REPRESENTATIVE ELEMENTARY VOLUME

Crack tensor theory by Oda (1986)

(1) Description of Crack Geometry

To introduce the characteristics of the discontinuities, the Crack tensor theory is employed, which gives an equivalent continuum model by using the geometry and properties of the fractures.

Let us consider that a representative elementary volume is homogeneously cut by $m^{(v)}$ cracks whose centers are distributed at random. Then, the density of the centers is expressed by

$$\rho = \frac{m^{(v)}}{V} \quad (10)$$

in which V is a representative elementary volume. Here, a discontinuity is assumed to have a representative diameter r and aperture t . Moreover, let \mathbf{n} be a unit normal vector to a discontinuity with components n_i with respect to axes, x_i ($i=1,2,3$). \mathbf{n} is oriented over the entire solid angle Ω corresponding to the surface of a unit sphere. For simplicity, (\mathbf{n}, r, t) discontinuities are used if the discontinuities are characterized by the following; the unit vectors \mathbf{n} are oriented inside a small solid angle $d\Omega$ around \mathbf{n} and the diameters and apertures range from r to $r+dr$ and from t to $t+dt$. A pdf $E(\mathbf{n}, r, t)$ is introduced in such that $2E(\mathbf{n}, r, t) d\Omega dr dt$ gives the probability of (\mathbf{n}, r, t) discontinuities where the function is only defined over the half solid angle $\Omega/2$.

(2) Permeability Tensor

Water is assumed to flow only through discontinuities and rock matrix blocks are assumed to be impermeable. The apparent flow velocity v_i is given by taking the average of the local velocity $v_i^{(c)}$ over the associated discontinuity volume $V^{(c)}$:

$$v_i = \frac{1}{V} \int_V v_i dV = \frac{1}{V} \int_{V^{(c)}} v_i^{(c)} dV^{(c)} \quad (11)$$

Let dN be a number of (\mathbf{n}, r, t) discontinuities whose centers are located inside the flow region V . dN is given by multiplying the probability of (\mathbf{n}, r, t) discontinuities by the total number $m^{(v)}$.

Assuming that the each (\mathbf{n}, r, t) discontinuity has a void volume of $(\pi/4)r^2t$, the total void volume $dV^{(c)}$ associated with (\mathbf{n}, r, t) discontinuities becomes

$$dV^{(c)} = \frac{\pi}{4} r^2 t dN = \frac{\pi}{2} m^{(v)} r^2 t E(\mathbf{n}, r, t) d\Omega dr dt. \quad (12)$$

Next consider the flow velocity suitable for (\mathbf{n}, r, t) discontinuities. Let $\mathbf{J}^{(c)}$ be the head gradient along an (\mathbf{n}, r, t) discontinuity. If overall head gradient \mathbf{J} is uniformly distributed over the entire flow region, $J_i^{(c)}$ is given by

$$J_i^{(c)} = (\delta_{ij} - n_i n_j) J_j \quad (13)$$

where n_i and J_i respectively are components of \mathbf{n} and \mathbf{J} projected on the orthogonal reference axes, x_i . The summation convention is adopted if any subscript appears twice.

If the water movement can be idealized by laminar flow between parallel planar plates with an aperture t , the local fluid velocity $v_i^{(c)}$ along the discontinuity is assumed to be given by

$$v_i^{(c)} = \frac{t^2 J_j}{12\mu} \quad (14)$$

where the so-called cubic law is employed.

Using equations (12), (13) and (14), (11) becomes

$$v_i = \frac{1}{12\mu} \left\{ \frac{\pi\rho}{4} \int_0^{l_m} \int_0^{r_m} \int_{\Omega} r^2 t^3 (\delta_{ij} - n_i n_j) E(\mathbf{n}, r, t) d\Omega dr dt \right\} J_j. \quad (15)$$

From this equation, an equivalent permeability tensor k_{ij} is obtained by

$$k_{ij} = \frac{1}{12\mu} (P_{kk} \delta_{ij} - P_{ij}) \quad (16)$$

where

$$P_{ij} = \frac{\pi\rho}{4} \int_0^{l_m} \int_0^{r_m} \int_{\Omega} r^2 t^3 (\delta_{ij} - n_i n_j) E(\mathbf{n}, r, t) d\Omega dr dt. \quad (17)$$

This integration form can be rewritten by the additive form. Thus, the crack tensor can be easily made from the measured fracture geometry data. However, this additive process may not be valid theoretically for the media having the randomly distributed fractures of which length is finite. Oda showed that the crack tensor theory can realize the anisotropic permeability tensor similar to the one made by the discontinuous approach by

Long, et al. (1982). Thus, this theory may be practically applicable to the general fractured media.

Although aperture, t , is used in the tensor P_{ij} , it is difficult to measure an aperture value at a field survey as a matter of fact. So, in the presented approach, the permeability tensor is rewritten as

$$k_{ij} = \frac{\alpha_{ij}^3}{12\mu} (Q_{kk}\delta_{ij} - Q_{ij}) \quad (18)$$

where

$$Q_{ij} = (\pi\rho/4) \int_0^m \int_{\Omega} r^2 n_i n_j E(n,r) d\Omega dr. \quad (19)$$

Q_{ij} is the tensor made by the fracture geometry except for aperture and is used to examine the dependency of the permeability on the volume. On the other hand, α_{ij} is the apparent aperture for the representative elementary volume and is related to the connectivity of the void and the aperture distribution in the volume. α_{ij} is obtained by using Q_{ij} for the representative elementary volume as

$$\alpha_{xx} = \sqrt[3]{\frac{12\mu k_{xx}}{Q_{yy} + Q_{zz}}}, \quad \alpha_{yy} = \sqrt[3]{\frac{12\mu k_{yy}}{Q_{xx} + Q_{zz}}}, \quad \alpha_{zz} = \sqrt[3]{\frac{12\mu k_{zz}}{Q_{xx} + Q_{yy}}}. \quad (20)$$

As a real process, Q_{ij} is calculated with the additive form like

$$Q_{ij} = \frac{\pi}{4} \left(\sum_{k=1}^M r^{k2} n_i^k n_j^k \right) / V \quad (21)$$

where M is the total number of the fracture in the volume, which is given as

$$M = \rho V. \quad (22)$$

Application to HRL Test Site

Using the theory mentioned above, the representative elementary volume at HRL site is examined. The fracture density used in the examination is obtained from the log normal function. The mean fracture length and the standard deviation are shown in Table 3. To calculate Q_{ij} , the following assumptions are also employed;

- 1) The position of the center of the fracture is according to the Poisson's distribution

- 2) The dip of fracture is according to the normal distribution
- 3) A fracture is truncated at the boundary of a volume
- 4) The number of the realizations is 50 and the mean value is obtained as Q_{ij} for the volume. Q_{ij} is calculated by the different initial random number.

Q_{ij} is calculated by adding the generated fractures in the volume according to the equation (21). The representative elementary volume is examined by changing the volume. Figure 5 shows the result of the examination of the representative elementary volume. It is seen from this figure that the representative elementary volume at the Äspö site is about a cube with side 30m.

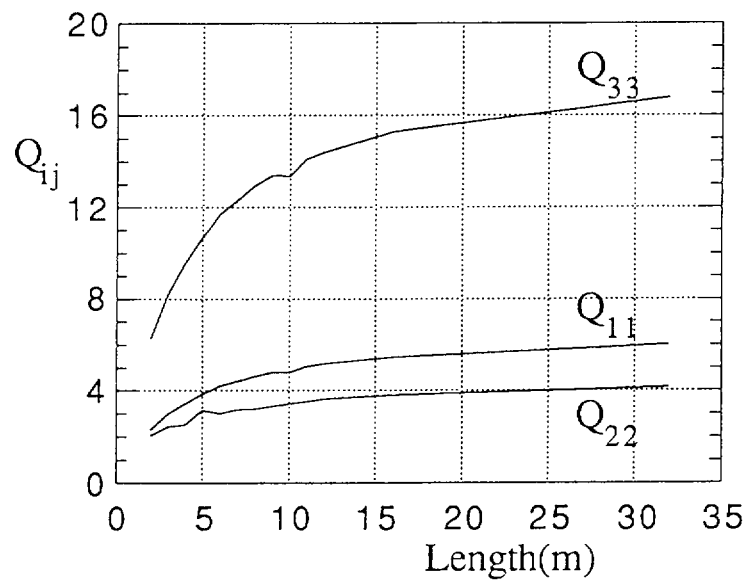


Figure 5 Q_{ij} as a function of the volume

Estimation of α_{ij}

As a next step, α_{ij} is estimated with Q_{ij} for the representative elementary volume. The permeability tensor components, k_{ij} , are used in the equation (20), which are obtained from the single borehole tests. In many cases, the permeability is calculated from a single borehole test by assuming the radial flow on the plane normal to the borehole direction and an imaginary boundary condition.

Therefore, if the borehole is inclined, the direction in which the permeability is calculated is different from the one in the case of a vertical hole. Thus, the permeability of the inclined borehole is expected to be different from the one of a vertical hole because of the difference of the direction of the hydraulic gradient subjected in the test. However, the permeability is treated as a constant value at the measured point without considering such

a difference between vertical and inclined holes in many approaches with geostatistics. This may be because the isotropy of the permeability is assumed in many cases.

In the presented approach, the permeability for the interval corresponding to the side length of the above representative elementary volume is used to estimate the permeability tensor components. The permeability for the side length of the representative elementary volume is calculated by using the arithmetic and geometric means of the permeability obtained from 3 m interval test. Comparing calculated pressure change with measured one, it is judged which averaging method is suitable for this region for an effective parameter. The permeability is assumed for the value on the plane normal to the borehole direction because water is expected to flow in the radial direction from the borehole. Thus, the permeability tensor can be written by using the local coordinate system, of which x' - y' plane is corresponding to the plane normal to the borehole and z' direction is the upward direction of the borehole. Figure 6 shows the schematic view of the concept. By using this local coordinate, the permeability tensor is written as

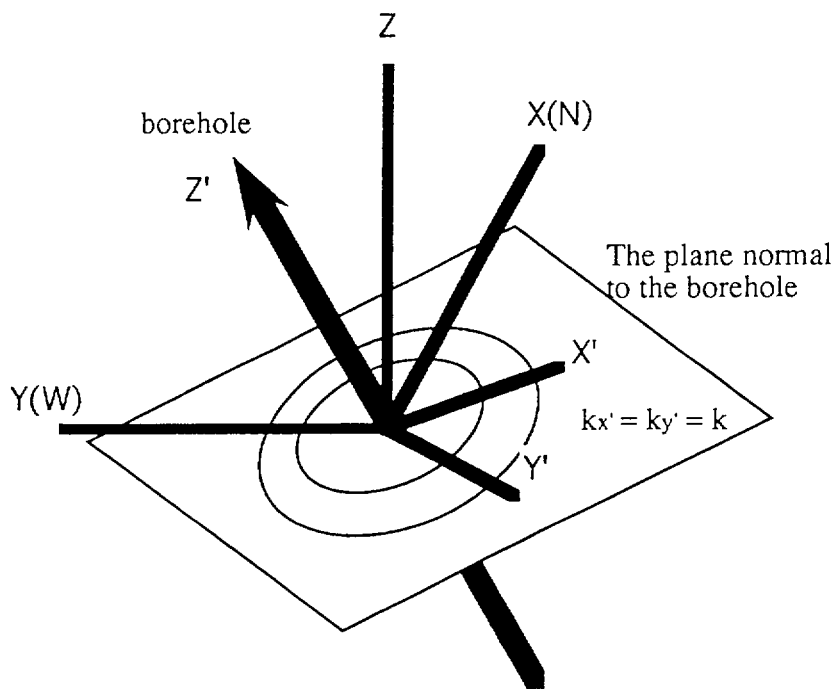


Figure 6 Schematic view of the coordinate

$$[k_{ij}] = \begin{bmatrix} k & 0 & 0 \\ 0 & k & 0 \\ 0 & 0 & 0 \end{bmatrix} \quad (23)$$

in which k is the permeability averaged for the interval length corresponding to the REV. This assumption does not mean that the value of k is the principal values. If each values of the components of the permeability tensor can be estimated from the test, the equation (23) may become an anisotropic matrix.

The transform matrix to the global coordinate system is obtained from the borehole direction vector. The borehole direction is given as

$$\mathbf{b} = (\sin \theta \cos \lambda, \sin \theta \sin \lambda, \cos \theta) \quad (24)$$

where θ is the angle between Z and Z' shown in Figure 6, λ is the angle between the direction of the trend of the borehole and the north, which is corresponding to X -coordinate in the global coordinate. Using the borehole direction, the transform matrix is given as

$$[T] = \begin{bmatrix} \cos \theta \cos \lambda & \sin \lambda \cos \theta & -\sin \theta \\ -\sin \lambda & \cos \lambda & 0 \\ \cos \lambda \sin \theta & \sin \theta \sin \lambda & \cos \theta \end{bmatrix} \quad (25)$$

The transform is carried out by the following equation;

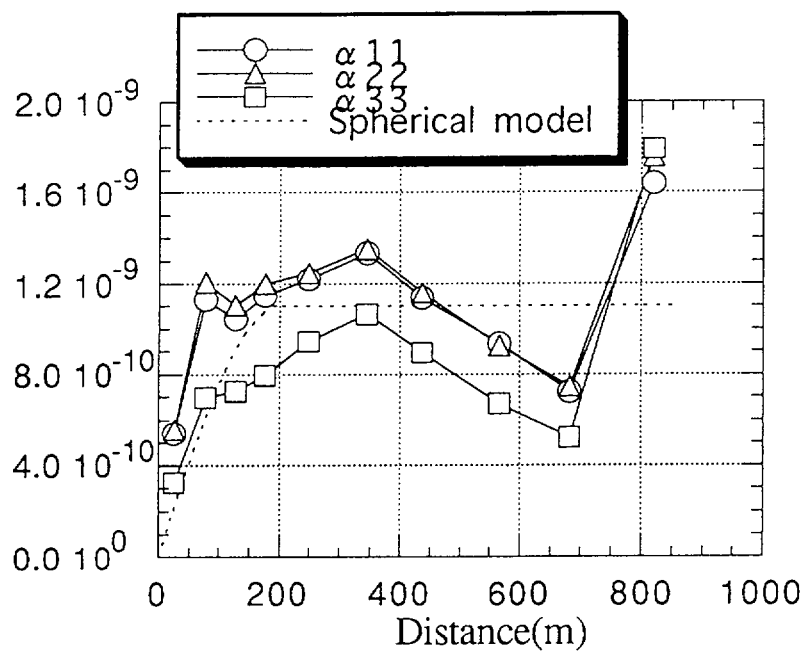
$$[k_{ij}] = [T][k_{ij}][T] \quad (26)$$

The permeability tensor transformed by the above equation is substituted into the equation (20), and α_{ij} are calculated.

Then, the variogram of α_{ij} is calculated. Figure 7 shows the variogram of α_{ij} for Äspö site. It is notable that the information of the vertical permeability is not so large in many cases because of difficulty to set the horizontal boreholes. Thus, the value of k_{zz} becomes small in the above process. The variogram of α_{33} is also not so stable as shown in Figure 7. To avoid the influence of the bias of the data and to reduce the influence of the assumption used in the equation (23), α_{ij} are assumed to be isotropic in this process and $\alpha_{ij}/3$ is assumed to be the representative value of α . The spherical model of the variogram for the mean value is also shown in Figure 7, of which equation is given as

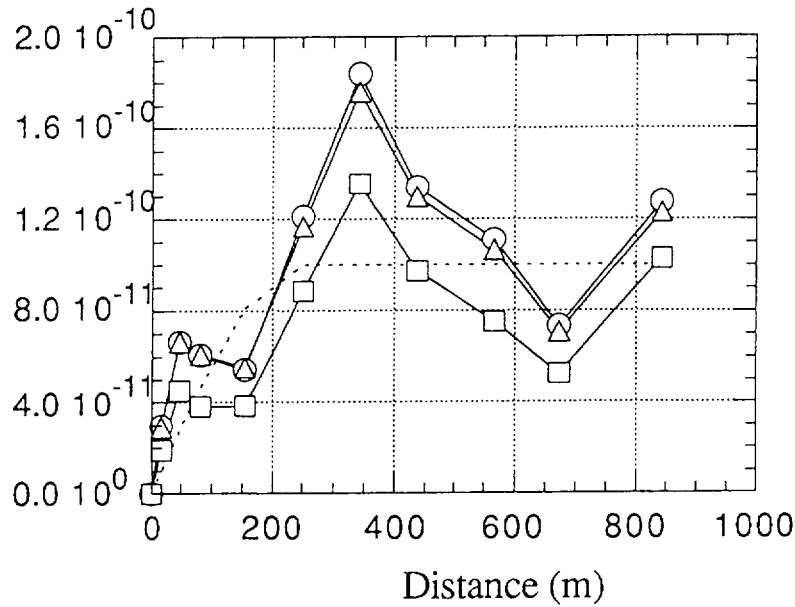
$$\begin{aligned}
 h > a; \omega & \left[\frac{3(h)}{2(a)} - \frac{1}{2} \left(\frac{h}{a} \right)^3 \right], \\
 h > a; \omega & \\
 \omega = 1.1 \times 10^{-9}, a = 200 & \text{ for arithmetic mean} \\
 \omega = 1.0 \times 10^{-10}, a = 300 & \text{ for geometric mean}
 \end{aligned}
 \tag{27}$$

where h is the distance (m). Using this spherical models and the calculated $\alpha_{ij}/3$ for each borehole, the heterogeneous α is realized by using the conditional simulation method of geostatistics. The simulation method used in the process is the three-dimensional turning bands method with moving average. α is assumed to follow a log normal distribution.



a) Arithmetic mean

Figure 7 Variogram of α_{ij}



b) Geometric mean

Figure 7 Variogram of α_{ij} (continued)

SEEPAGE AND TRANSPORT ANALYSES

Model Description

The analysis region is shown in Figure 8, at which center a series of boreholes used in the tracer test exist. The finite element mesh should be smaller than the REV because the heterogeneous effect of macro-permeability appears in the larger volume. The REV for HRL test site is estimated as the 30m cube and so the region is divided into the element volume of 30m cube as shown in Figure 9. The certain fracture zones, i.e., EW1, EW3 and NE2, are deterministically modeled by the two-dimensional plane elements, of which permeability is given with the mean value estimated from the field experiments because the number of the measurement points is too small to apply the geostatistics to introduce the heterogeneous permeability distribution. The other possible fracture zones, i.e., a series of NNW and EW5, are modeled as a rock block by using the equivalent continuum approach mentioned above. The permeability in the rock blocks is given as the heterogeneous field by distributing the apparent aperture α to each element by a conditional simulation while the anisotropy induced by the Crack tensor theory is homogeneous. The total number of nodes used in the analyses is 14,508.

The flow analyses are carried out by a steady state condition because the tracer test was conducted by using the steady state of the ground water flow. The vertical

boundaries are assumed to be prescribed pressure condition and the top and bottom boundaries are assumed to be no-flow condition. In the analyses, the precipitation is not considered. Pumping up at KAS06 is simulated by giving the sink condition to the nodes corresponding to the locations where inflow rate is measured by the spinner survey, as shown in Figure 10.

Since the heterogeneous field is considered as a random process in the analyses, many realizations have to be produced and the mean results have to be compared with the measured values. The dispersion phenomenon is modeled as the random process of the heterogeneous path of the solute particles. Thus, the breakthrough curve at the observed hole is modeled by summing up the results of all realizations. The path of a solute from each injection point is traced with the velocity field for each realization. The solute particle will flow into the pumping up hole because of the radial convergency flow condition. The arrival time of a solute is calculated for each realization and the breakthrough curve is obtained as a collection of particles having different arrival time. The concentration of a given interval Δt is calculated from

$$C_{\Delta t} = \sum_{n=1}^N C_n^{\Delta t} / F_{\Delta t} \quad (28)$$

where $C_n^{\Delta t}$ is the concentration of the particle, $F_{\Delta t}$ is the total pumping up rate in Δt and N is the total number of arriving particles during Δt . Δt is the interval between t_i and t_{i+1} and $C_{\Delta t}$ is plotted as the concentration at $(t_i+t_{i+1})/2$.

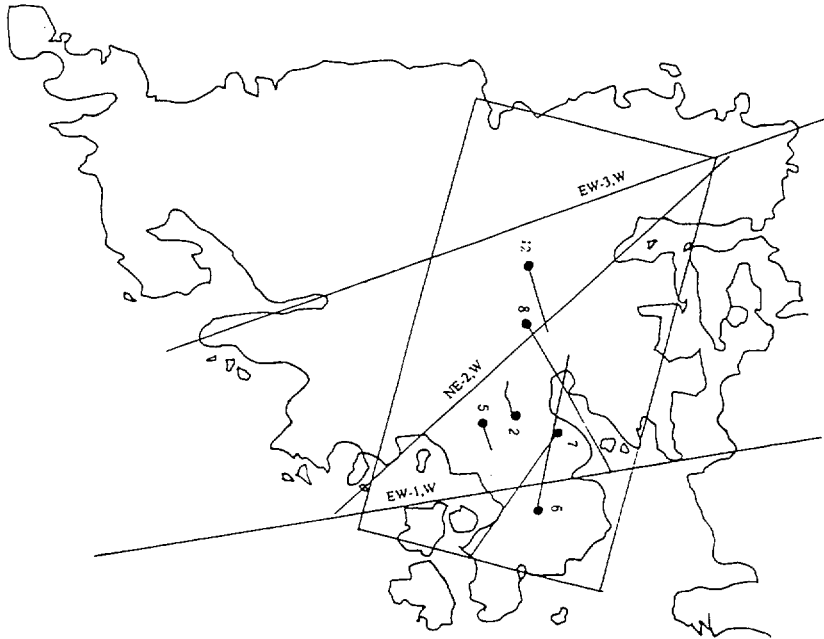


Figure 8 Analysis region

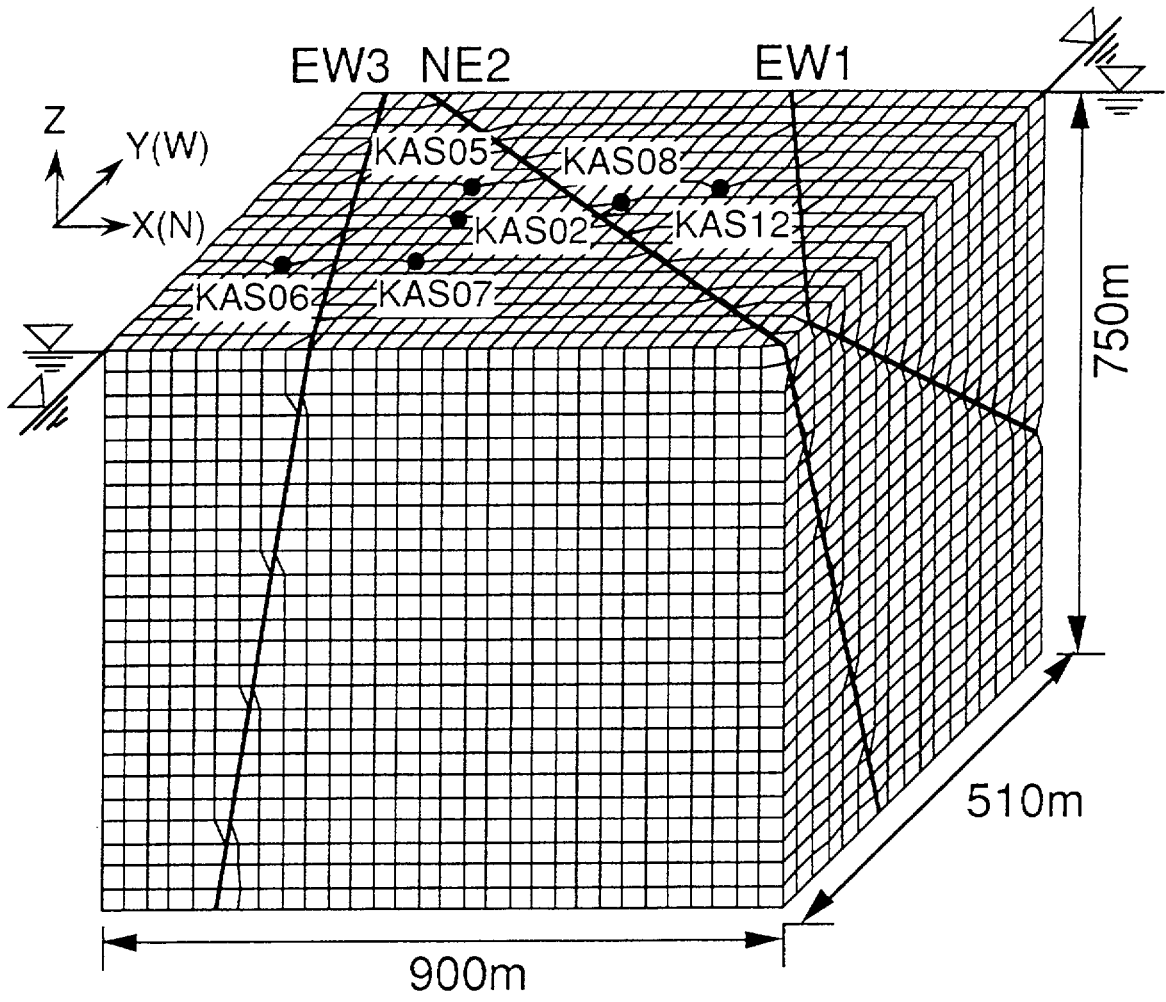


Figure9 Finite elment mesh

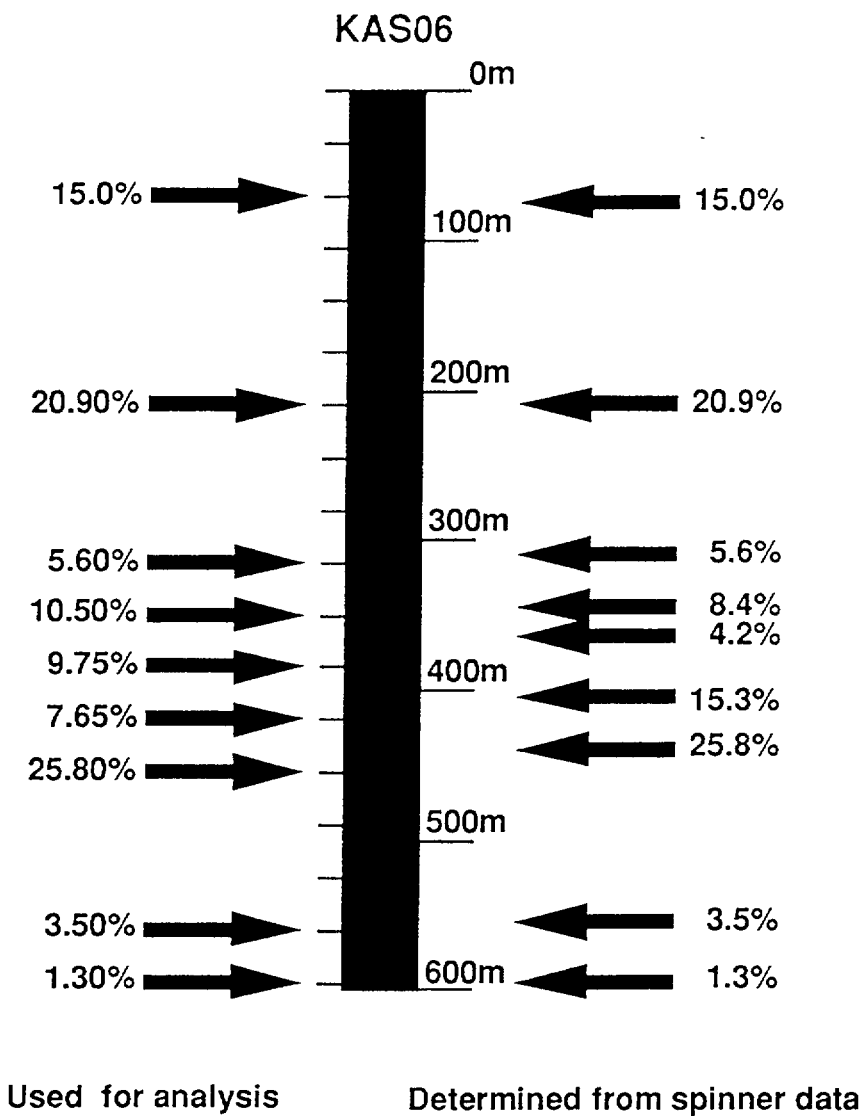


Figure 10 Inflow rate at KAS06

Results of Flow Analyses

Figure 11 shows the comparison between calculated and measured drawdown at each observation boreholes. In this model, KAS 2, 5, 7, 8 and 12 are modeled. These results are obtained from the analyses with the permeability derived from the arithmetic mean of the measured results. When the geometric mean is used for the permeability in the equation (20), the drawdown becomes over a few meters at the observed boreholes and a few hundreds meters at the withdrawal borehole. This is because the permeability is estimated very small value. On the other hand, the drawdown obtained from the arithmetic mean permeability has a relatively good agreement with the measured one. This means the arithmetic mean is better than the geometric mean to obtain the effective parameters for this site. Figure 12 shows the mean drawdown distribution along KAS06. The drawdown does not become same along the borehole because the high conductivity

of the borehole of KAS06 is not considered in the model. The maximum drawdown is 66m and the mean one is 27m.

Table 5 shows the same result as Figure 11. The error between measured and calculated drawdown has a large variation. In particular, KAS07 has a large variation along the depth.

Table 6 shows the comparison of the calculated flow rate into the holes with the measured ones. It is found that the measured flow rates are larger than the calculated ones. The calculated maximum flow rates has a relatively good agreement with the measured ones. The flow rate for each location is calculated by multiplying the velocity of the nodes corresponding to the measurement points by the sectional area of the hole. This discrepancy between calculation and measurement may be caused from the good connectivity of the high permeability region near the measurement points in the real filed. However, it would be necessary for reproduction of such a heterogeneity of small area to obtain more detail observation near the measurement points. The smaller fractures than fractures zones, NNW and EW5, have to be modeled.

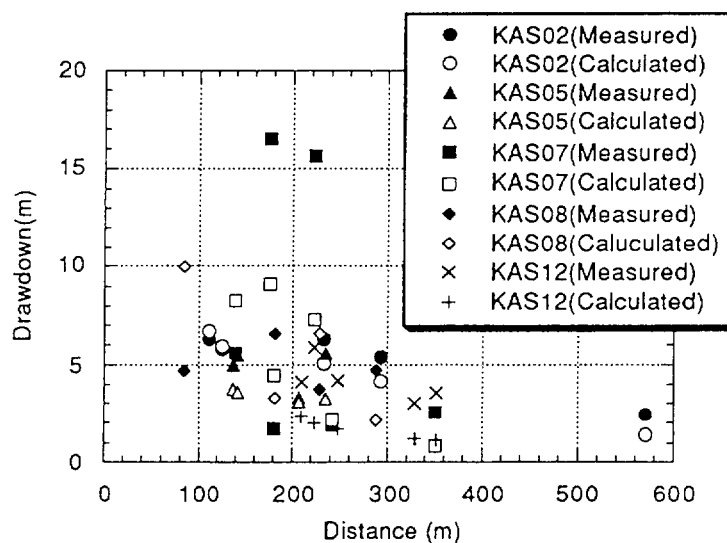


Figure 11 Comparison between calculated and measured drawdown

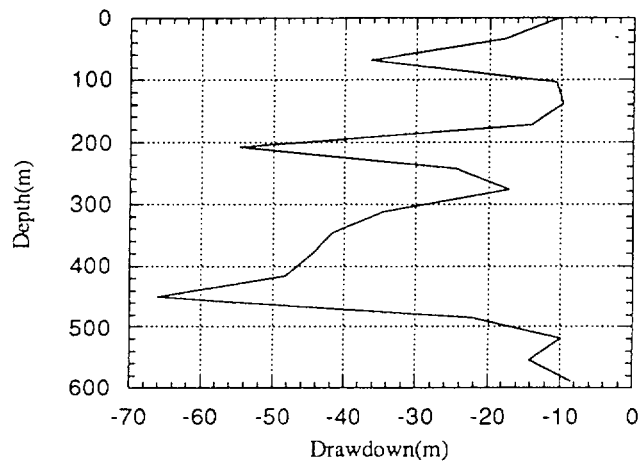


Figure 12 Drawdown distribution at KAS06

Table 5 Comparison between calculated and measured drawdown

Borehole	DEPTH(m)	R(m)	PMEAS(m)	PCALC(m)	ERROR(m)
KAS02,B6	52.00	233.00	-6.30	-5.05	-1.25
KAS02,B5	189.00	125.00	-5.79	-5.93	0.14
KAS02,B4	309.00	111.00	-6.30	-6.72	0.42
KAS02,B3	537.00	293.00	-5.40	-4.17	-1.23
KAS02,B2	824.00	571.00	-2.41	-1.39	-1.02
KAS02,B1	873.00	619.00	-2.30	-1.31	-0.99
KAS05,E5	81.00	235.00	-5.58	-3.24	-2.34
KAS05,E4	263.00	137.00	-4.97	-3.75	-1.22
KAS05,E3	312.00	142.00	-5.45	-3.57	-1.88
KAS05,E2	426.00	207.00	-3.30	-3.08	-0.22
KAS05,E1	456.00	230.00	-3.06	-2.86	-0.20
KAS07,J6	47.00	223.00	-15.64	-7.28	-8.36
KAS07,J5	104.00	176.00	-16.53	-9.10	-7.43
KAS07,J4	206.00	139.00	-5.61	-8.26	2.65
KAS07,J3	295.00	181.00	-1.69	-4.47	2.78
KAS07,J2	363.00	242.00	-1.88	-2.18	0.30
KAS07,J1	470.00	351.00	-2.54	-0.82	-1.72
KAS08,M4	52.00	288.00	-4.73	-2.13	-2.60
KAS08,M3	147.00	182.00	-6.58	-3.28	-3.30
KAS08,M2	314.00	84.00	-4.70	-9.97	5.27
KAS08,M1	455.00	229.00	-3.74	-6.57	2.83
KAS12,DE	88.00	352.00	-3.54	-1.11	-2.43
KAS12,DD	116.00	329.00	-3.00	-1.20	-1.80
KAS12,DC	228.00	248.00	-4.20	-1.70	-2.50
KAS12,DB	279.00	223.00	-5.87	-1.98	-3.89
KAS12,DA	345.00	210.00	-4.13	-2.32	-1.81

Table 6 Flow rate at boreholes

Borehole	flow rate (ml/min)			
	Measured	Calculated		
		mean value	standard deviation	MAX
KAS02,B4	2.00	0.53	0.57	3.77
KAS02,B2	4.00	0.11	0.23	2.67
KAS05,E3	9.00	0.93	0.96	7.66
KAS05,E1	11.00	0.92	1.01	7.36
KAS07,J4	18.00	2.21	2.50	26.34
KAS08,M3	21.00	0.48	0.60	3.79
KAS08,M1	48.00	5.13	2.68	24.36
KAS12,DB	107.00	0.45	0.77	8.07

Results of Transport Analyses

As mentioned above, the dispersion phenomenon is considered to be caused from the heterogeneous velocity field and the heterogeneity of the permeability is modeled as a random process. The concentration of the particle is given by dividing the total concentration by the total number of the realizations. Firstly, to compare the measured results, the effective porosity is calibrated for the first arrival time of the particle. The porosity is given by the Crack tensor theory as

$$n = \frac{V_c}{V} = \rho \int_0^{r_m} \int_0^{r_m} \int_{\Omega} \frac{\pi r^2 t E(\mathbf{n}, r, t)}{4} d\Omega dr dt = \frac{\pi \alpha \overline{r^2}}{4} \quad (28)$$

where $\overline{r^2}$ is the expected value of the square of the fracture length. Thus, the porosity of an element is given as a non uniform distribution. The effective porosity is calibrated by multiplying the same factor by the porosity of each element. As a result, the factor of 10 is used to calculate the breakthrough curve.

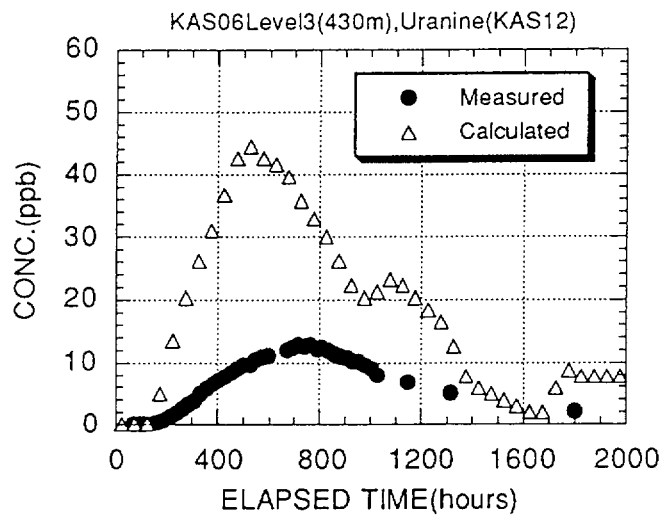
Moreover, although the total number of the realizations is about 200, the number of the particles is not so enough to calculate the smooth breakthrough curve. The concentration is calculated by dividing the total concentration of the particles by the total pumping up rate during an interval. Thus, the concentration is dependent on the interval to calculate the concentration if the enough number of particles are not given. In this case, the number of the realization is not enough and so the interval is calibrated for the breakthrough curve till the effect of the interval becomes small and the breakthrough

curve becomes smooth. As a result, the interval of 50 hours are used to draw the breakthrough curves.

Figure 13 shows the comparison between calculated and measured breakthrough curves for the test in which the tracer is injected from KAS12. It is found that the result for the depth of 390m has a good agreement with the measured one.

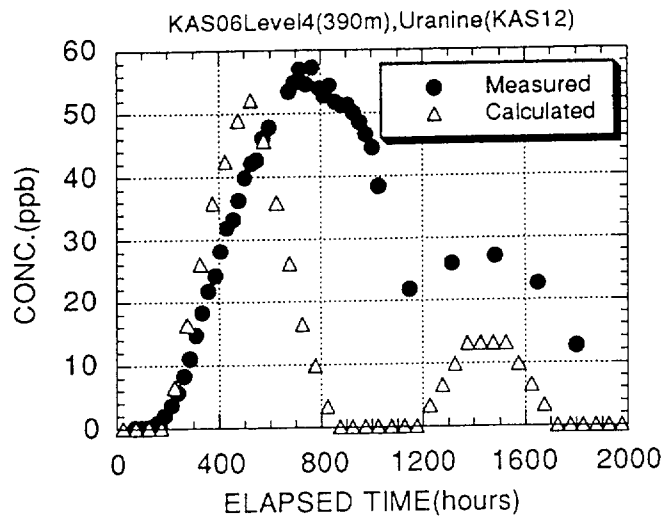
Figure 14 shows the comparison for the test in which the tracer is injected from KAS08. The measured results at the depth of 360m and 290m are strange because the concentration becomes negative value. These phenomena cannot be reproduced by the numerical calculations. The calculated results have larger concentration than the measured ones.

As mentioned above, the tracers from the other holes are moved into the pumping-up hole in the calculation because the numerical simulation is carried out to minimize the lost particles. Except for KAS08-3, all the tracer from the other holes are moved into KAS06 and the breakthrough curve can be drawn. Figure 15 shows the result for the tracer from KAS05. If all the tracer are recovered in the field and the concentration of the stagnant tracers are measured, the model could consider such a phenomenon.

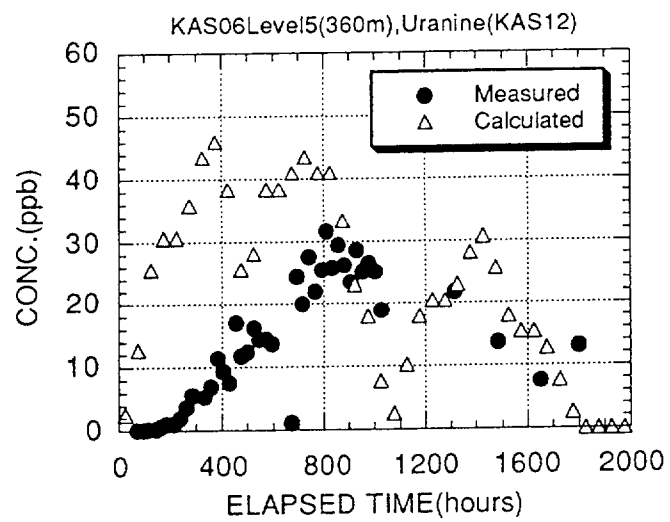


(a) Comparison of the level 13(430m)

Figure 13 Calculated and measured breakthrough curve for the test from KAS12

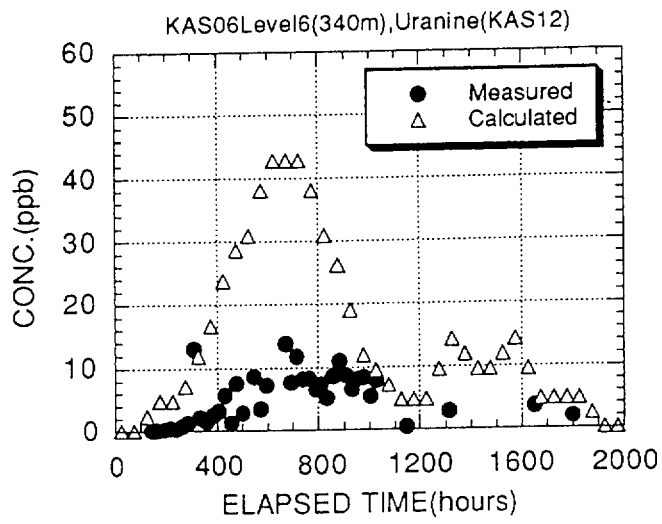


(b) Comparison of the level 14 (390m)

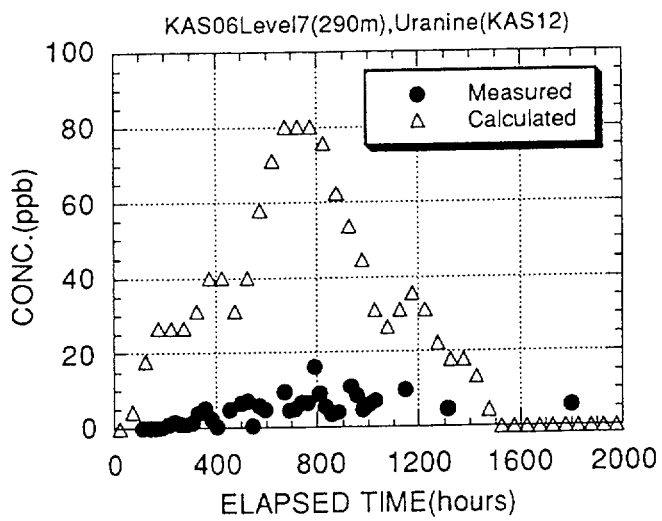


(c) Comparison of the level 15(360m)

Figure 13 Calculated and measured breakthrough curve for the test from KAS12 (continued)

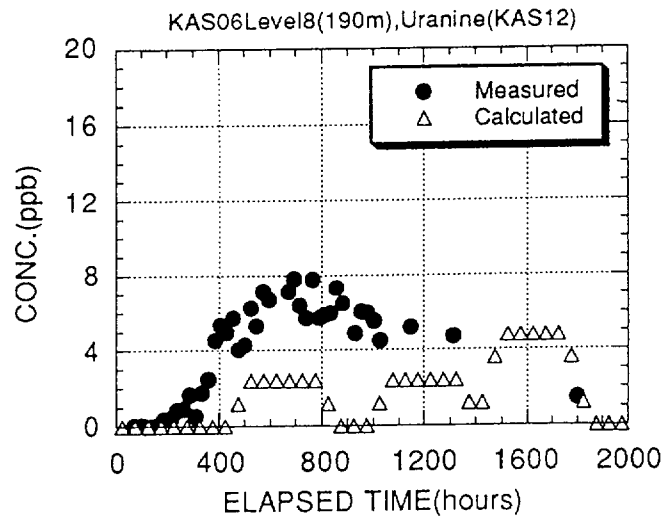


(d) Comparison of the level 16(340m)

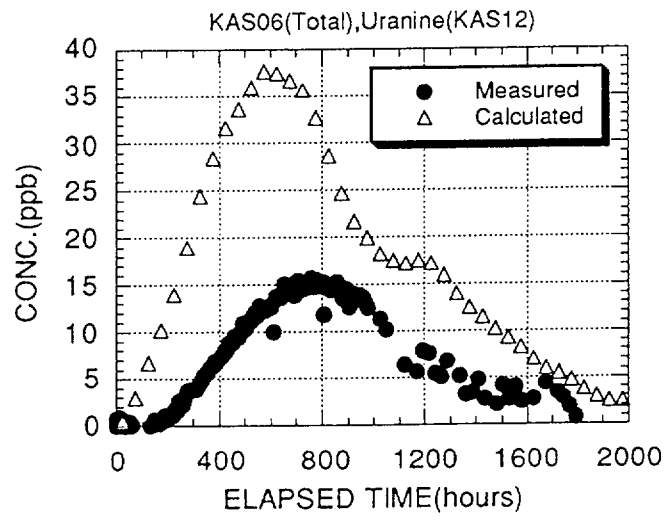


(e) Comparison of the level 17(290m)

Figure 13 Calculated and measured breakthrough curve for the test from KAS12 (continued)

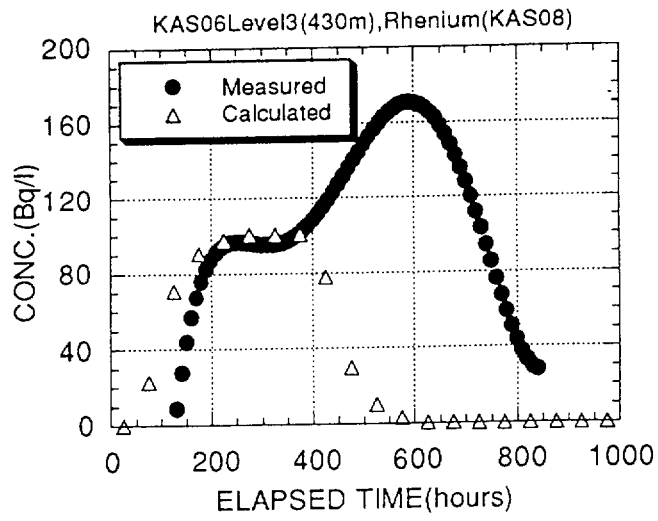


(f) Comparison of the level 18(190m)

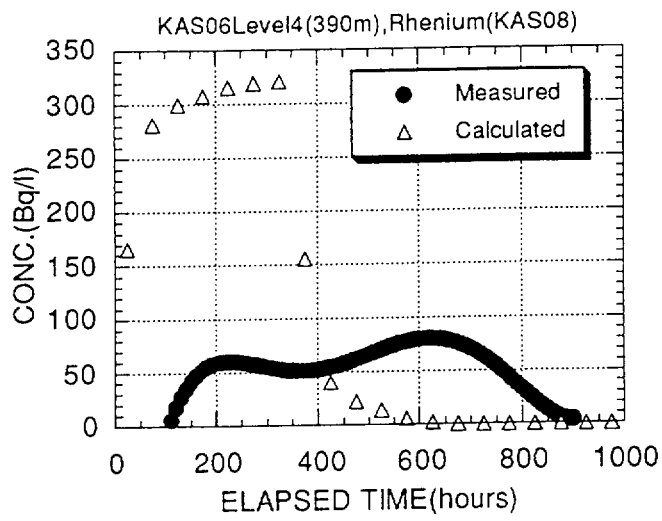


(g) Comparison of the total concentration

Figure 13 Calculated and measured breakthrough curve for the test from KAS12 (continued)

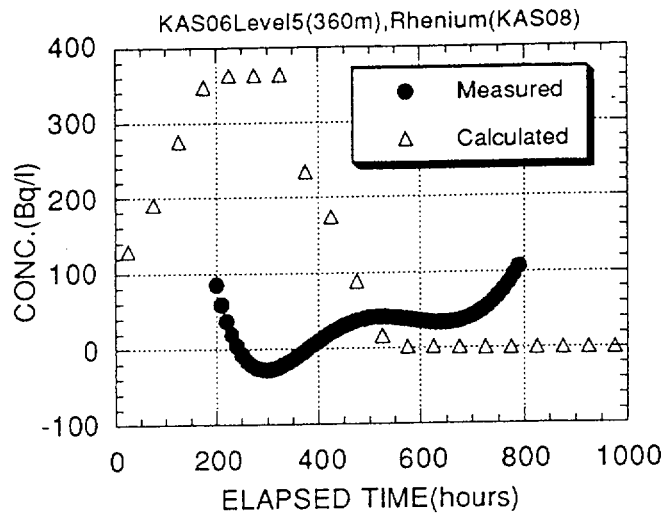


(a) Comparison of the level 13 (430m)

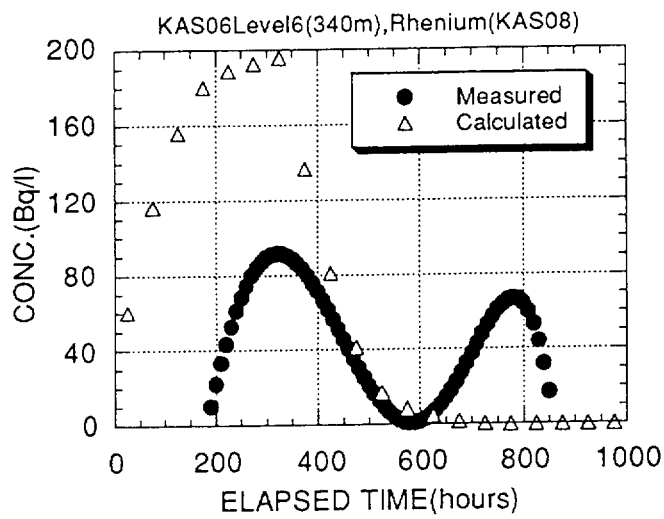


(b) Comparison of the level 14 (390m)

Figure 14 Calculated and measured breakthrough curve for the test from KAS08

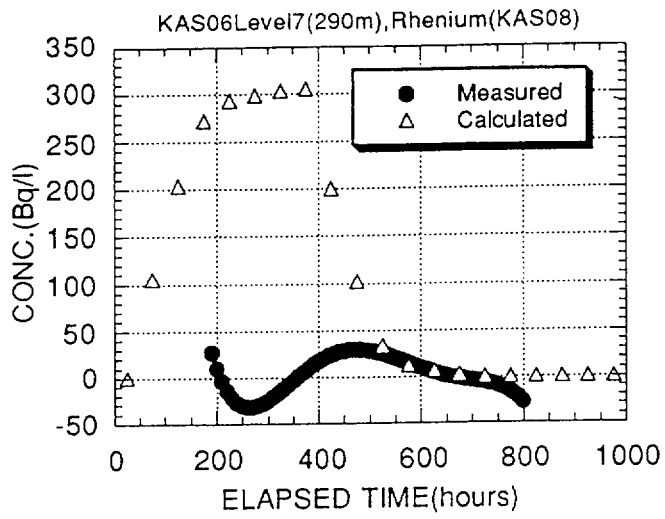


(c) Comparison of the level 15 (360m)

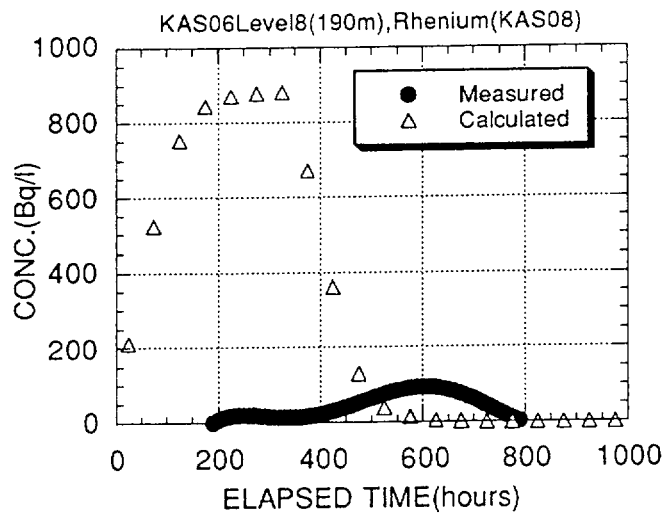


(d) Comparison of the level 16 (340m)

Figure 14 Calculated and measured breakthrough curve for the test from KAS08 (continued)



(e) Comparison of the level 17 (290m)



(f) Comparison of the level 18 (190m)

Figure 14 Calculated and measured breakthrough curve for the test from KAS08 (conitnued)

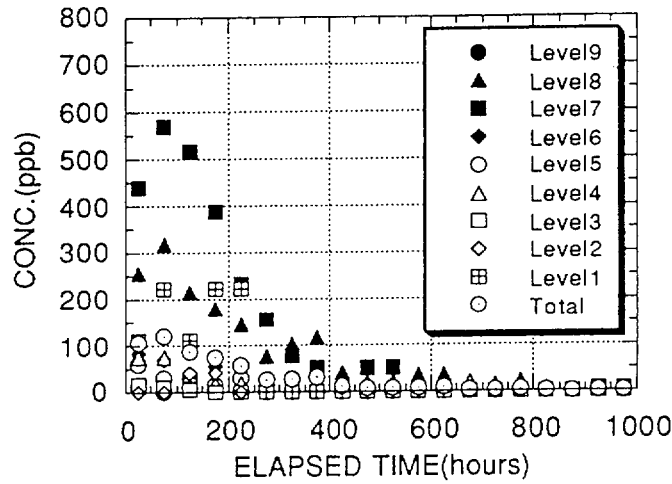


Figure 15 Calculated breakthrough curve from KAS05

DISCUSSION AND CONCLUSIONS

The effect of the magnitude and deviation of the velocity direction on the solute transport is modeled in the presented approach by the anisotropic heterogeneous permeability in the flow analyses. To avoid the dependency of the mesh size on the permeability distribution, we use the same mesh size as the representative elementary volume, which is estimated from the Crack tensor theory. The permeability has to be fundamentally defined from the solution of the boundary values problem. So, the permeability has the meaning for the volume which the problem is defined in, e.g., the laboratory tests and the field tests. The volume which the permeability is not sensitive for is called a representative elementary volume. In many fractured media, the representative elementary volume may not be so small because of the complicated fracture network system and biased flow in the region. It may be difficult in such a case that the permeability is considered as the value at a point and that the permeability is isotropic. Thus, the heterogeneous approach considering the anisotropy and the representative elementary volume is important for a flow analysis in fractured media. The mechanical dispersion phenomena can be understood to be caused from the heterogeneous velocity vector distribution due to the heterogeneous permeability field. Since a macro-dispersion phenomenon is expressed by the random process in the model, the breakthrough curve is calculated by the ensemble of the arrival time of the particles of each realized model. The molecular diffusion and the mechanical dispersion due to the heterogeneity of the velocity in smaller region could be considered in the model. However, those phenomena are not

considered in the model because of the ambiguity and uncertainty of the understanding of those phenomena. The phenomena excluding from the present model should be examined with the fact of the low recovery of the tracer.

The main assumptions used in the analysis can be summarized as follows;

- 1) The large certain fracture zones, i.e., EW3, NE2 and EW1, can be presented by two dimensional plane elements of which location is decided according to the conceptual model. A series of NNW fracture zones and EW5, the probably confirmed fracture zones, can be modeled by the equivalent continuous approach.
- 2) The Crack tensor theory can be used for modeling of Äspö site. Moreover, the REV can be assumed to exist.
- 3) The boundary condition, i.e., prescribed pressure condition for vertical boundaries and no flow condition for top and bottom boundaries, can be assumed
- 4) The steady state of flow can be assumed.
- 5) The molecular diffusion can be negligible and the mechanical dispersion can be presented as a random process of heterogeneous velocity field.

The results of our approach can be summarized as follows;

- 1) The pdf of the fracture length is estimated to be a log normal distribution. The mean and standard deviation of the fracture length for each set are estimated as shown in Table 3. The fracture density for each set is also indicated in Table 3. These results are obtained from the process shown in Figure 4 by using the results of geological survey.
- 2) The representative elementary volume of the Äspö area is estimated to be about 30m cube. Thus, the finite element mesh has to be made with the smaller volume than 30m cube.
- 3) It is better that the permeability measured at a single borehole test is averaged with an arithmetic mean rather than the geometric mean. This may mean the good connectivity of the high permeability region because the measured high permeability has much effect on the permeability of the volume of REV.
- 4) The drawdown of the head measured at observation holes are well simulated by the calculation with the permeability averaged with an arithmetic mean. When the permeability from the geometric mean is used, the drawdown is estimated too much.
- 5) The flow rate through a hole is underestimated by the calculation. The calculated maximum flow rate has a better agreement with the measured results. This may mean the good connectivity pattern of the high permeability near the borehole had better be realized more carefully.
- 6) In our approach, the concentration is calculated by dividing the total concentration of the particles reaching in a given interval time by the total flow rate in the interval. Thus, if the number of the particle is small and the interval is short, the calculated

concentration becomes very high and the coarse discontinuous curve is obtained. To avoid this difficulty, the interval is set to be 50 hours and the number of the realization is about 200. So, it is difficult to estimate the recovery of the tracer in the model, which is dependent on the number of the realizations and the interval time to measure the concentration. If the number of the realizations is enough and the measured concentration is considered to be the averaged one for one hour, the recovery of the tracer in the model can be estimated by 2%. It is impossible to compare with the measured concentration during an instant period. The breakthrough curve calculated by the above approach has a relatively good agreement with the measured ones. However, the breakthrough curve can be calculated for the tracer which was not measured in the field because the tracer is moving into the pumping-up hole in the simulation.

REFERENCES

- Dershowitz, W., P. Wallmann and S. Kindred, 1991, Discrete Fracture Modeling for the Stripa Site Characterization and Validation Drift Inflow Prediction, Stripa Project Technical Report, SKB
- Herbert, A. and B. Splawski, 1990, Prediction of inflow into the D-holes at the STripa mine, Stripa Project TR 90-14, SKB
- Oda, M, 1986, An Equivalent Continuum Model for Coupled Stress and Fluid Flow Analysis in Jointed Rock Masses, Water Resour. Res., Vol. 22, No. 13, pp. 1845-1856

Appendix A

Model and Code Specification

Name, version and origin of the code

SETRA (SEepage flow and TRAJectory analyses code)

The version number is 1.0

ARRANG (ARRANGing code to calculate the breakthrough curve with the resulting data from SETRA)

The version number is 1.1

General description

SETRA code is constructed by three parts. One is a code to calculate the heterogeneous permeability field with conditional simulation, the second one is a steady flow analysis code and the third one calculates the travel time of a particle from injection point to observed point by using the velocity field. The initial random number is changed for each realization automatically and the number of realization is set as input data.

After using SETRA, ARRANG is used to calculate the breakthrough curve by using the trajectory record from SETRA. The transport porosity and the interval of concentration calculation are calibrated with this code.

Conceptual and mathematical model

The governing equation of the flow analyses is written as

$$\frac{\partial}{\partial x_i} \left(k_r k_{ij} \frac{\partial h}{\partial x_j} \right) + Q = 0$$

where h is the total head, k_r is the relative permeability to saturated one, k_{ij} is the saturated permeability tensor and Q is the sink/source term. The saturated permeability is calculated in the code so that

$$k_{ij} = \frac{\alpha^3}{12\mu} (Q_{kk} \delta_{ij} - Q_{ij})$$

where α is the apparent aperture and Q_{ij} is the crack tensor. α is calculated for each element by using a conditional simulation in the code. The Q_{ij} is given as input data. The rectangular finite element is automatically divided into six tetrahedrons and the velocity field is calculated for each element by using the

result of total head filed. The travel time of a particle is calculated according to the specification of the tracer experiment and the arrival time of a particle at the observation point is obtained for each realization.

The concentration of breakthrough curve is calculated by

$$C_{\Delta t} = \sum_{n=1}^N C_n^{\Delta t} / F_{\Delta t}$$

where $C_n^{\Delta t}$ is the concentration of the particle, $F_{\Delta t}$ is the total pumping up rate in Δt and N is the total number of arriving particles during Δt . Δt is the interval between t_i and t_{i+1} and $C_{\Delta t}$ is plotted as the concentration at $(t_i+t_{i+1})/2$.

Numerical method

Galerkin finite element method is used for discretization. Any shape of an element can be used and the element is divided into tetrahedron elements in the code. A linear shape function is used. The plane and line elements can be also used to present the discontinuous structure.

Limitation

Unsteady analyses is not considered in the code because many realizations have to be analyzed.

Unsaturated region is not considered.

However, this code is originally an unsteady saturated-unsaturated flow analysis code and modified for the analyses of HRL and Finnsjön cases. Thus, it will be easy to remove above limitations if necessary.

Parameters required

for SETRA

Mesh data

Boundary condition

Crack tensor values

The number of realizations

The points of injection and observation

The inferred variogram of the apparent aperture

for ARRANG

Transport aperture

Interval time in which the concentration is calculated for breakthrough curve

Type of results

- Total head at each node
- Velocity at each element and node
- Travel time from injection to observation point

Computer requirement

FORTRAN 77 compiler is necessary.

User interface

The data for a post processor code is made and the total head distribution and velocity vector distribution can be seen on a screen.

Appendix B

Main data used in the model

Type of data from Äspö	Affecting model input parameter
Fracture orientation (PR25-89-16)	Classification of fracture sets
Fracture data in boreholes distributed in FD	fracture density and length
Fracture data on outcrops distributed in FD	fracture density and length
K data(3 m) distributed in FD	apparent fracture aperture
Spinner survey at KAS06	sink condition at KAS06

List of International Cooperation Reports

ICR 93-01

Flowmeter measurement in
borehole KAS 16

P Rouhiainen

June 1993

Supported by TVO, Finland

ICR 93-02

Development of ROCK-CAD model
for Äspö Hard Rock Laboratory site

Pauli Saksa, Juha Lindh,

Eero Heikkinen

Fintact KY, Helsinki, Finland

December 1993

Supported by TVO, Finland

ICR 93-03

Scoping calculations for the Matrix
Diffusion Experiment

Lars Birgersson¹, Hans Widén¹,
Thomas Ågren¹, Ivars Neretnieks²,
Luis Moreno²

1 Kemakta Konsult AB, Stockholm,
Sweden

2 Royal Institute of Technology,
Stockholm, Sweden

November 1993

Supported by SKB, Sweden

ICR 93-04

Scoping calculations for the Multiple
Well Tracer Experiment - efficient design
for identifying transport processes

Rune Nordqvist, Erik Gustafsson,
Peter Andersson

Geosigma AB, Uppsala, Sweden

December 1993

Supported by SKB, Sweden

ICR 94-01

Scoping calculations for the Multiple
Well Tracer Experiment using a variable
aperture model

Luis Moreno, Ivars Neretnieks
Department of Chemical Engineering
and Technology, Royal Institute of
Technology, Stockholm, Sweden

January 1994

Supported by SKB, Sweden

ICR 94-02

**Äspö Hard Rock Laboratory. Test plan for
ZEDEX - Zone of Excavation Disturbance
EXperiment. Release 1.0**

February 1994

Supported by ANDRA, NIREX, SKB

ICR 94-03

**The Multiple Well Tracer Experiment -
Scoping calculations**

Urban Svensson

Computer-Aided Fluid Engineering

March 1994

Supported by SKB, Sweden

ICR 94-04

**Design constraints and process discrimination
for the Detailed Scale Tracer Experiments at Äspö -
Multiple Well Tracer Experiment and Matrix Diffusion
Experiment**

Jan-Olof Selroos¹, Anders Winberg²,
Vladimir Cvetkovic²

1 Water Resources Eng., KTH

2 Conterra AB

April 1994

Supported by SKB, Sweden

ICR 94-05

Analysis of LPT2 using the Channel Network model

Björn Gylling¹, Luis Moreno¹,

Ivars Neretnieks¹, Lars Birgersson²

1 Department of Chemical Engineering
and Technology, Royal Institute
of Technology, Stockholm, Sweden

2 Kemakta Konsult AB, Stockholm, Sweden

April 1994

Supported by SKB, Sweden

ICR 94-06

**SKB/DOE geochemical investigations using stable and
radiogenic isotopic methods - First year**

Bill Wallin¹, Zell Peterman²

1 Geokema AB, Lidingö, Sweden

2 U.S. Geological Survey, Denver, Colorado, USA

January 1994

Supported by SKB and U.S.DOE

ISSN 1104-3210
ISRN SKB-ICR--94/7--SE
CM Gruppen AB, Bromma 1994